Validation of spectroscopic data in the 1.27 μm spectral region by comparisons with ground-based atmospheric measurements

D.D. Tran, T. Delahaye, Raymond Armante, J.-M. Hartmann, D. Mondelain, A. Campargue, H. Fleurbaey, J.T. Hodges, H. Tran

Validation of spectroscopic data in the 1.27 μm spectral region by comparisons with ground-based atmospheric measurements

D. D. Tran[1], T. Delahaye[2], R. Armante[2], J.-M. Hartmann[2], D. Mondelain[3], A. Campargue[3], H. Fleurbaey[4], J. T. Hodges[4], H. Tran[1,*]

[1]*Laboratoire de Météorologie Dynamique, IPSL, CNRS, Sorbonne Université, École Normale Supérieure, PSL Research University, École Polytechnique, Institut Polytechnique de Paris, F-75005 Paris, France*
[2]*Laboratoire de Météorologie Dynamique, IPSL, CNRS, Ecole Polytechnique, Institut polytechnique de Paris, Sorbonne Université, Ecole Normale Supérieure, PSL Research University, F-91120 Palaiseau, France*
[3]*Univ. Grenoble Alpes, CNRS, LIPhy, 38000 Grenoble, France*
[4]*Material Measurement Laboratory, National Institute of Standards and Technology, 100 Bureau Drive, Gaithersburg, MD 20899, USA*

Abstract:
Various spectroscopic data for absorption lines due to the magnetic dipole transitions of the $a\ ^1\Delta_g - X\ ^3\Sigma_g^-(0-0)$ band of O_2 centered at 1.27 μm are tested by comparison with high-resolution ground-based atmospheric measurements recorded by Fourier Transform Spectrometers at Park Falls and Caltech (USA). This band is of importance for atmospheric remote sensing since it will be used (together with the O_2 A-band near 760 nm) by the passive short wave infrared spectrometer onboard the MicroCarb satellite mission (i.e. this band includes the B4 band of MicroCarb, from about 7800 cm^{-1} to 7912 cm^{-1}) for the determination of surface pressure and atmospheric aerosols. Spectroscopic data of the HITRAN2016 and GEISA2015 databases as well as those from recent laboratory studies are here used in a radiative transfer code to simulate atmospheric transmissions under the conditions of the measurements. Comparisons are made for different solar zenith angles and for the whole B4 spectral range considered by MicroCarb. Spectroscopic data of water vapor are also tested by considering both relatively dry and humid atmospheric conditions. Averaging the "calculated-observed" residuals over numerous recordings made for close values of the solar zenith angle and humidity enables reduction of the uncertainties due to the radiometric noise of the instrument and to the imperfect description of the atmospheric state. This enables the detection of systematic differences in the spectral residuals caused by small changes in spectroscopic data. The results show that the spectroscopic parameters in the HITRAN2016 and GEISA2015 databases lead to large residuals while data of two recent laboratory studies, obtained from spectra measured with the cavity ring-down spectroscopy technique using the speed-dependent Nelkin-Ghatak profile lead to much better agreement with atmospheric measurements.

* Corresponding author: ha.tran@lmd.jussieu.fr

Significant residuals are noted for water vapor absorption lines simulated using parameters provided by both the HITRAN and GEISA databases.

1. Introduction

O_2 absorption plays an essential role in the determination of air-mass and remote sensing calibration (e.g. [1-6]) because the volume-mixing ratio of atmospheric oxygen is well known (0.2095) and uniformly distributed. When compared to the commonly-used A-band near 0.76 μm, the 1.27 μm band is closer to the CO_2 and CH_4 bands (near 1.61 μm, 1.67 μm and 2.06 μm) which are used by various greenhouse gas remote sensing experiments (e.g. [3,7-9]). Due to atmospheric scattering, atmospheric path lengths vary with the aerosols' load, their vertical distribution and their optical properties. The spectral distance between the O_2 A-band and the CO_2, CH_4 bands results in significant uncertainties due to the varying spectral properties of the aerosols. There should be less uncertainty when using the O_2 band at 1.27 μm as a proxy of the atmospheric path length to the CO_2 and CH_4 bands. The 1.27 μm band is used by the Total Carbon Column Observing Network (TCCON) [2] and the Collaborative Carbon Column Observing Network (COCCON) [10] for ground-based air-mass determinations. Thanks to recent and accurate modeling of the strong mesosphere/stratosphere airglow produced by O_3 photo-dissociation [4,6], this band will be probed by the satellite mission MicroCarb, to be launched in 2021, dedicated to the accurate determination of column integrated concentrations of CO_2 [9]. The spectrometer on board MicroCarb will collect the solar irradiance scattered by the surface (and aerosols) in four spectral ranges corresponding to the O_2 A-band (B1) around 0.76 μm, the two CO_2 bands around 1.6 μm (B2) and 2 μm (B3), and the O_2 band at 1.27 μm (B4) [9].

The O_2 1.27 μm band consists of narrow absorption lines of the $a\,^1\Delta_g - X\,^3\Sigma_g^-(0-0)$ transition superimposed over a much broader collision-induced absorption (CIA) structure due to the dipole induced in short-lived collisional O_2-O_2 and O_2-N_2 complexes. Several spectroscopic studies were devoted to the latter system. The HITRAN2016 database [11] provides the CIA coefficients derived from high-pressure spectra measured at several temperatures with a Fourier transform spectrometer by Maté *et al.* [12]. Theoretical calculations, scaled according to [12], were also reported by Karman *et al.* [13,14]. Room temperature CIA binary coefficients were recently determined with improved accuracy, from low density spectra [i.e. from (0.97 to 2.3)×10^{19} molecule/cm^{-3} equivalent to 0.36 to 0.85 amagat] of pure oxygen and of an O_2/N_2 mixture by highly sensitive cavity ring-down

spectroscopy (CRDS) [15]. Despite the lower sample pressures used in this CRDS study, the retrieved CIA coefficients were found in very good agreement with the FTS values by Maté *et al.* [12].

The absorption lines of the 1.27 μm band were investigated in various studies. In HITRAN2016, the line positions were calculated by differences between the energy levels of the $a\ ^1\Delta_g(0)$ and $X\ ^3\Sigma_g^-(0)$ states reported by Yu *et al.* [16]. The intensities for the magnetic dipole transitions were calculated by Orr-Ewing on the basis of the FTS values of [17], while air-broadening and -shifting coefficients were set to those obtained for the A-band in [2] and [18]. In GEISA2015 [19], most of the line parameters are the same as in HITRAN2016 except for some weak lines corresponding to quadrupolar transitions. Only Voigt line-shape parameters are provided by HITRAN2016 and GEISA2015. Recently, some studies showed that the Voigt profile leads to significant deviations from measured spectra for the 1.27 μm band lines [5,20-22] and that the speed dependence of the collisional broadening and the collision-induced velocity changes have to be taken into account. Using the quadratic speed-dependent Voigt (qsdV) profile to fit high sensitivity CRDS air-broadened spectra of 97 O_2 lines in the 1.27 μm band, Mendonca *et al.* [5] obtained fit residuals largely improved with respect to the Voigt profile. In [5], the line positions were fixed according to HITRAN2012 [23], while the line intensities and line-shape parameters were obtained from fits of CRDS spectra. More recently, positions and intensities of 170 lines including very weak electric quadrupole transitions were reported in the 7920-8085 cm^{-1} interval [24]. The reported line parameters were retrieved from low pressure (0.67 kPa and 1.34 kPa) spectra of pure O_2 measured with a CRDS setup based on an extended cavity diode laser (ECDL) and coupled to a self-referenced frequency comb using the quadratic speed-dependent Nelkin-Ghatak profile (qsdNG). A CRDS setup using a series of distributed feedback laser diodes and referenced to the same frequency comb was used to record air- and N_2-broadened spectra of O_2 in the 7800-7912 cm^{-1} region corresponding to the B4 band of MicroCarb [25]. Line intensities and line-shape parameters were retrieved for 85 O_2 magnetic lines using the qsdNG model [25]. Line-mixing (LM) between lines in the *Q* branch was taken into account with the use of the first order line-mixing approximation [26]. In parallel, Fleurbaey and Hodges [27] also studied the absorption spectrum of O_2 in this spectral region using a frequency-stabilized cavity ring down spectrometer. Spectroscopic parameters for 99 magnetic lines were determined in the 7797-7953 cm^{-1} range from air-broadened spectra measured at room temperature. The qsdNG model

together with the first order line-mixing approximation were used to analyze the measurements [27].

Compared to the HITRAN2016 and GEISA2015 lists, significant differences between the line positions, intensities and shape parameters have been pointed out in these recent CRDS studies (see [24,25] for instance). In the present work, different spectroscopic datasets of the $a\ ^1\Delta_g - X\ ^3\Sigma_g^-(0-0)$ band [5,11,19,24,25,27] are tested by comparing ground-based atmospheric transmission measurements (TCCON spectra) with spectra calculated using the Spectroscopic Parameters And Radiative Transfer Evaluation (SPARTE) chain [28]. The TCCON spectra were chosen for these validation tests since they provide a high signal-to-noise ratio and high resolution together with well-known pressure, temperature and humidity conditions as well as instrument characteristics (see [3] and references therein). The SPARTE chain is a calibration/validation chain used to compare ground-based and space-borne observations with atmospheric spectra simulated from direct radiative transfer calculations based on the 4A/OP code [29]. The latter has been selected for calibration/validation activities of MicroCarb. The remainder of this paper is divided into three sections. Section 2 is dedicated to the presentation of the spectroscopic data and atmospheric measurements used and to the calculation procedure. Comparisons between calculated and measured atmospheric spectra are then discussed in Section 3, before some concluding remarks and directions for future studies (Section 4).

2. Spectroscopic data, atmospheric measurements used and method of calculations

2.1 Spectroscopic data used

Table 1 lists the five sets of spectroscopic parameters for O_2 in the 1.27 μm spectral region used for comparisons with ground-based atmospheric spectra.

Dataset	Refs.	Profile used
HITRAN	[11]	V
GEISA	[19]	V
Mendonca2019	[5]	qSDV
Tran2020	[25]	qSDNG+LM
Fleurbaey2020	[27]	qSDNG+LM

Table 1: Summary of the considered datasets for the O_2 absorption lines of the 1.27 μm band.

The first one, hereafter called "Tran2020", includes data from Tran *et al.* [25] from 7784.8 cm^{-1} to 7915.8 cm^{-1} retrieved from CRDS spectra recorded for a large pressure range from 6.7 to 94 kPa (50 to 700 Torr) and fitted with the qsdNG profile. For Q branch lines, first order line-mixing (LM) effects were also taken into account. Within this model, the absorption coefficient α at wavenumber σ for a transition is given by:

$$\alpha(\sigma) = Sn_{O_2}[\mathrm{Re}\{I^{qsdNG}(\sigma)\} - Y\ \mathrm{Im}\{I^{qsdNG}(\sigma)\}]. \quad (1)$$

In this equation, Y is the first-order line-mixing parameter, representing the coupling between the considered transition and other lines. S and n_{O_2} are the line intensity (at natural isotopic abundance [11]) and the number density of oxygen, respectively. The area-normalized line-shape quantity $I^{qsdNG}(\sigma)$ is a function of seven parameters (see [30] for instance):

$$I^{qsdNG}(\sigma) = f(\sigma - \sigma_0, \Gamma_D, \Gamma_0, \Gamma_2, \Delta_0, \Delta_2, \nu_{vc}), \quad (2)$$

with σ_0 the line position, Γ_D the Doppler half-width and ν_{vc} the velocity-changing collision frequency. Γ_0, Δ_0 and Γ_2, Δ_2 characterize the collision-induced line width and shift and their speed dependence components, respectively [31,32]. Note that the air-broadening coefficients ($\gamma_0 = \Gamma_0/P$) of [25] were given at the temperature of the measurements (about 294 K). The corresponding values at room temperature (296 K) were thus deduced using the temperature dependence exponents given in HITRAN2016 [11].

The second set ("Fleurbaey2020") corresponds to the CRDS data of [27] for 99 O_2 lines in the 7797-7953 cm^{-1} region retrieved from air-broadened spectra measured at room temperature and various pressures, from 3.3 to 99 kPa (25 to 750 Torr). The same line-shape model as for "Tran2020" was used to fit the measured spectra except that the velocity changing frequency ν_{vc} was replaced by the modified form as proposed in [33].

In the third set ("Mendonca2019") the quadratic speed dependent Voigt (qsdV) profile was used to fit air-broadened spectra of 97 O_2 lines in the 7797-7940 cm^{-1} spectral region. This qsdV profile is obtained from Eq. (2) by simply fixing $\nu_{vc} = 0$.

For these three sets, the lower state energy of the transitions and the temperature dependence of the air-broadening coefficients were taken from HITRAN2016. The other line-shape parameters (i.e. pressure-shift coefficient, $\delta_0 = \Delta_0/P$, speed-dependent coefficients of the line broadening and shifting, LM and Dicke narrowing coefficients, ν_{vc}/P) were assumed to be independent of temperature. For the weak transitions missing in these various datasets (in particular, electric quadrupole transitions and lines of the minor isotopologues), their spectroscopic parameters were directly taken from HITRAN2016, thus employing the Voigt profile in the calculations. These three sets of data were used to model the O_2 absorption lines

and compared to simulations with HITRAN2016 ("HITRAN") and GEISA2015 ("GEISA") line lists (calculated with the Voigt profile).

Figure 1 shows the comparisons between the line positions, line intensities, air pressure-induced line shifting and broadening coefficients in "Mendonca2019", "Tran2020" and "Fleurbaey2020" and those provided in HITRAN2016. No comparison with data in GEISA2015 are reported here since they are identical to those of HITRAN2016. More detailed comparisons can be found in [25,27]. For the line positions and pressure shifts, there are systematic differences between HITRAN2016 and [5,25,27]. Good agreement is observed for [25] and [27] while there are systematic differences between these two and [5]. For the line-broadening coefficients and intensities, the HITRAN values are smaller than those of the three other datasets (about 2% for both γ_0 and S in average). Weak but systematic differences are also observed between the data of [5], [25] and [27]. Note that part of these observed differences could be due to the different line-shape models used to fit the measured spectra (i.e. "Tran2020" and "Fleurbaey2020" used the qsdNG, "Mendonca2019" used the qsdV while the Voigt profile is used with HITRAN data).

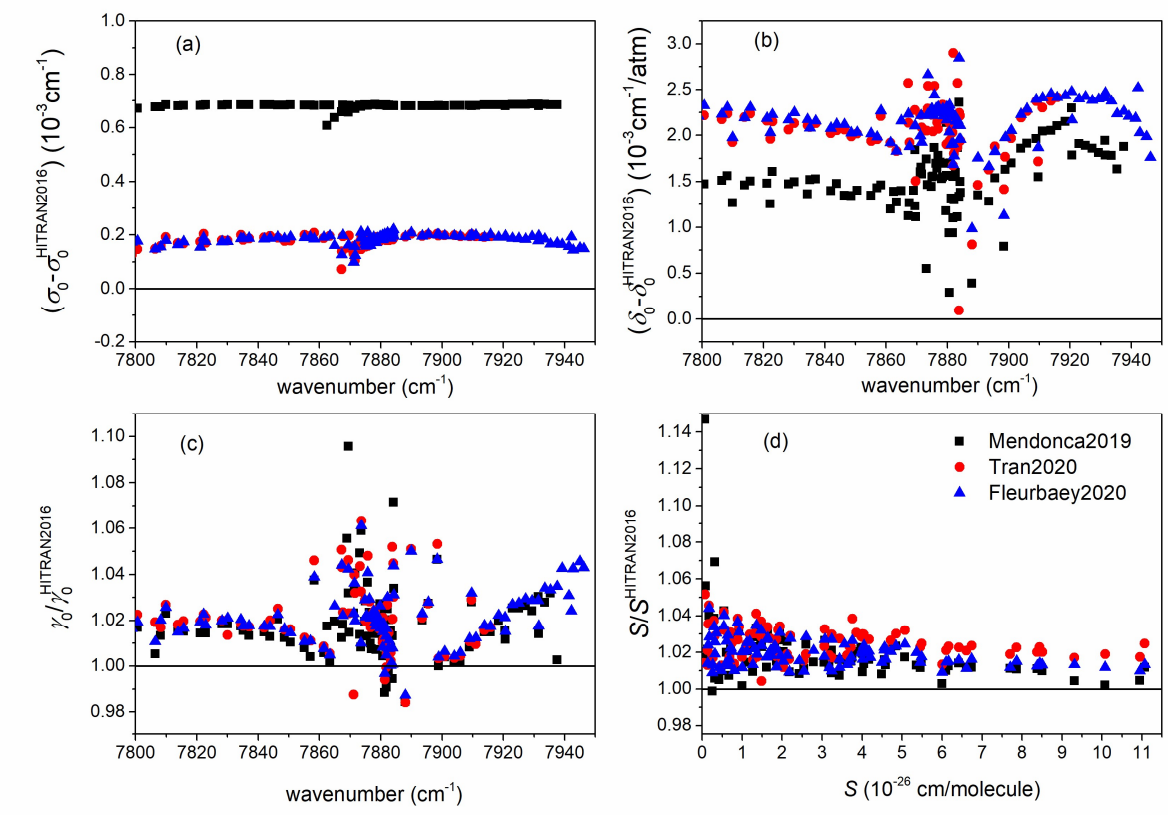

***Fig. 1** : Comparisons between line parameters of oxygen in the $a\ ^1\Delta_g - X\ ^3\Sigma_g^-(0-0)$ band, given in [5], [25] and [27] and those provided by the HITRAN2016 database, for line positions (a), air pressure-induced line shift coefficients (b), air-broadening coefficients (c) and line intensities (d).*

2.2 Atmospheric measurements and data used

TCCON spectra of the GGG2014 data version [34], which were corrected for solar intensity variations, phase error and laser sampling error, were used. Three sets of TCCON spectra were used in this study: two sets were used for the validation of the O_2 line lists while the third set, with high humidity conditions, were used to evaluate water spectroscopic data in this region. Each contains a large number of spectra with similar solar zenith angles and atmospheric humidity levels. They were recorded between October 2014 and September 2017 at Park Falls (Wisconsin, United States), and between October 2015 and April 2017 at Caltech (California, United States) using a Bruker 125 HR FTIR spectrometer for each station[*].

The first set contains 65 spectra, measured at Park Falls for relatively dry atmospheres [with total precipitable water (TPW) contents from 0.15 cm to 0.97 cm] with solar zenith angles ranging from 60° to 80°. The second set was recorded at the Caltech station and includes 40 spectra with solar zenith angles and humidity conditions similar to those of the first. The third set comprises 10 spectra measured at Park Falls with solar zenith angles of about 40° at relatively high humidity conditions (TPW≈2 cm). As shown below and in [28], the use of several spectra involving similar atmospheric conditions allows one to average the residuals, thus minimizing the random errors caused by both the radiometric noise of the instrument and the imperfect knowledge of the atmospheric state.

The atmospheric states used as inputs to the atmospheric transmission calculations were obtained from both NCEP/NCAR (National Centers for Environmental Prediction/National Center for Atmospheric Research) [35] and ERA-Interim [36] reanalyses products from ECMWF (European Centre for Medium-Range Weather Forecasts). Specifically, pressure, temperature and water profiles were taken from Era-Interim, corrected by local surface measures on TCCON site to take into account the differences in the space and time collocation. CO_2 (and also N_2O, CO and CH_4) profiles were taken from NCEP/NCAR and corrected by a scaling factor corresponding to the column abundance retrieved from each TCCON spectrum [34] These profiles are finally re-gridded on ERA-Interim pressure grid. The instrument spectral response functions were taken from [34] while information about the surface pressure, instrument altitude and solar zenith angle were taken from TCCON.

2.3 Calculation procedure

[*] Certain commercial equipment, instruments, or materials are identified in this paper in order to specify the experimental procedure adequately. Such identification is not intended to imply recommendation or endorsement by the National Institute of Standards and Technology nor is it intended to imply that the materials or equipment identified are necessarily the best available for the purpose.

The considered ground-based atmospheric transmission spectra were simulated using the five sets of spectroscopic data described in Sec. 2.1 but with the same model for the CIA. The latter corresponds to the recent data measured by Mondelain *et al.* [15] for values at room temperature. Their (small) temperature dependences were taken from Maté *et al.* [12] using:

$$\mathrm{CIA(T)} = \mathrm{CIA(296\ K)} * \frac{\mathrm{CIA\_X(T)}}{\mathrm{CIA\_X(296\ K)}} \quad (3)$$

where $\mathrm{CIA(296\ K)}$ is the coefficient given by Mondelain *et al.* at 296 K, $\mathrm{CIA\_X(T)}$ is the coefficient from Maté at *T*, derived through linear interpolation of values at different temperatures. The data relative to the O_2 CIA and lines were then implemented in the SPARTE chain [28] developed at Laboratoire de Météorologie Dynamique (LMD). In SPARTE, radiative transfer simulations are performed by using the 4A (Automatized Atmospheric Absorption Atlas) radiative transfer code. The full range of the B4 band of MicroCarb (7800-7912 cm^{-1}) is considered. For each set of O_2 spectroscopic line parameters, different line shapes were used, consistently with the profile used for their determination (see **Table 1**). Spectroscopic data for other absorbing species *i.e.* H_2O, CH_4 and CO_2, were taken from GEISA2015 [19]. The O_2 mole fraction was fixed at 20.95% of the dry-air content in the calculations. The solar contribution was taken from [37]. Calculations were performed for 40 atmospheric layers (from the ground to approximately 5 Pa). A global shift (about 0.0005 cm^{-1} depending on the spectrum and on the considered site) for the whole spectral range was determined for each measured spectrum. Except for a linear (*versus* wavenumber) multiplicative correction for the 100% transmission level, there are no other adjustable parameters in the calculations.

3. Validation tests and discussion

3.1 Spectroscopic line parameters of the O_2 $a\ ^1\Delta_g - X\ ^3\Sigma_g^-(0-0)$ band.

Comparisons with a single spectrum recorded on 15 January 2017 at the TCCON Park Falls station, under dry atmospheric conditions (TPW=0.37 cm) for a SZA of 68.16° are presented in **Fig. 2**. The corresponding "calculated-observed" residuals obtained with the five spectroscopic datasets are plotted in the lower panels, together with the root-mean-square (*rms*). The obtained results show relatively small improvements of "Mendonca2019", "Tran2020" and "Fleurbaey2020" with respect to HITRAN and GEISA, except for the Q branch region for which large differences in line parameters between HITRAN, GEISA and the three other datasets can be observed (see **Fig. 1** and **Fig. 6** of [25]). Note that this result is consistent with [5] which showed that the use of "Mendonca2019" dataset together with the qsdV profile leads

to only slightly better fit residuals than using the existing data in the TCCON standard analysis software GGG [34] with the Voigt profile. The three datasets "Mendonca2019", "Tran2020" and "Fleurbaey2020" lead to very similar residuals that are all within the noise level of the measured spectra.

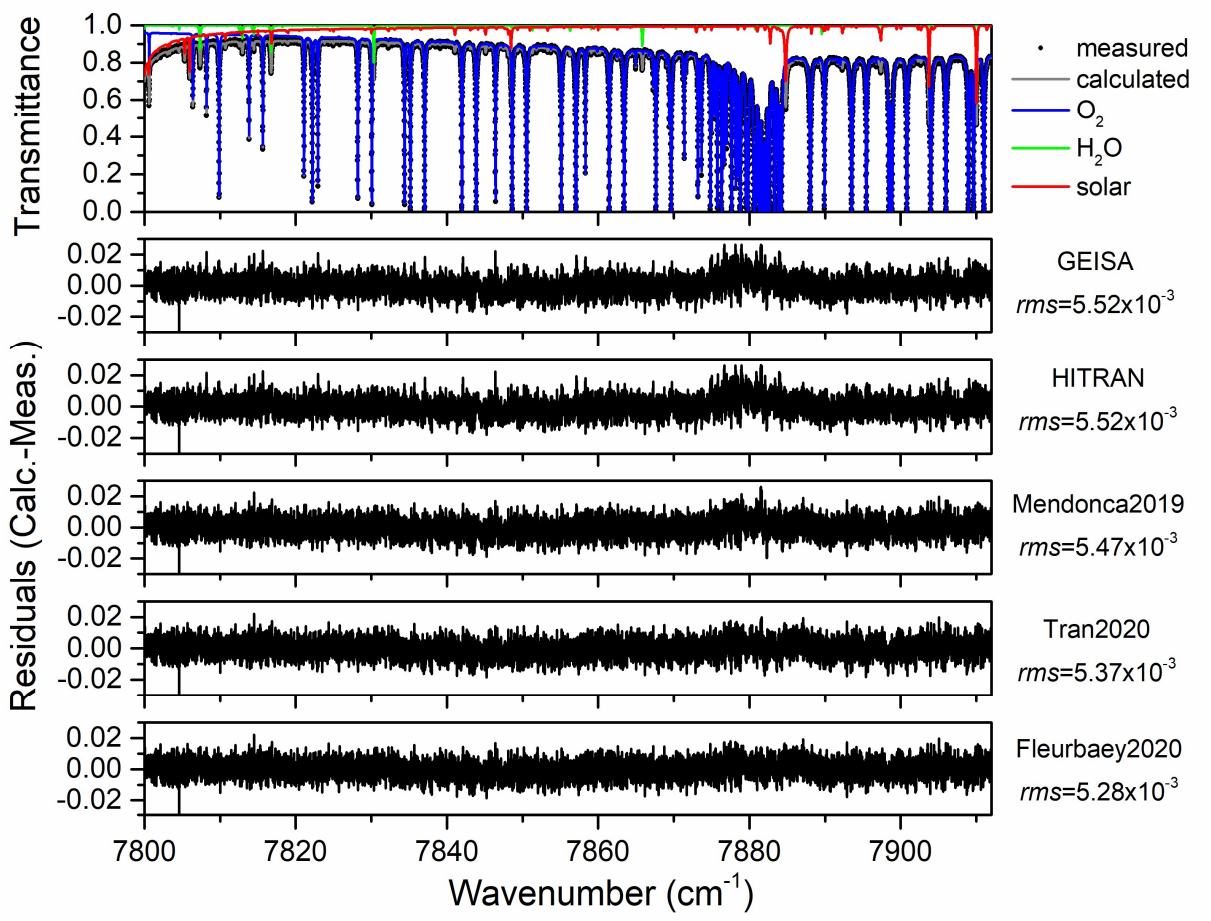

***Fig. 2**: Comparison between a dry spectrum, recorded on 15 January 2017 at the TCCON Park Falls station for a SZA of 68.16° in the B4 band of MicroCarb and simulations using various sets of spectroscopic data for the transitions of O_2 in the $a\ ^1\Delta_g - X\ ^3\Sigma_g^-(0-0)$ band (see Table 1). The upper panel shows the measured transmission, the corresponding simulated spectrum and the contribution of O_2 absorption obtained using the "Tran2020" list. In the lower panels are the corresponding "calculated-measured" residuals.*

In order to better distinguish results obtained with different datasets and reduce the influence of experimental noise and the random errors caused by uncertainties in the temperature and pressure profiles used, the residuals obtained for large number of spectra with close SZA and humidity conditions were averaged. The averaged residuals are shown in **Figs. 3** and **4**, respectively together with the corresponding *rms* values. Because results obtained with GEISA2015 are identical to those with HITRAN2016, they will be omitted from now on. As illustrated in **Fig. 2**, spectrum averaging reduces the random noise so that differences resulting

from the line parameters are revealed. We note that residuals obtained with 65 spectra recorded at Park Falls (**Fig. 3**) and those obtained with the 40 spectra recorded at Caltech (**Fig. 4**) are very similar showing the consistency of the results for these two stations. These results clearly show the improvement of the "Mendonca2019", "Tran2020" and "Fleurbaey2020" datasets with respect to HITRAN2016. In particular, the HITRAN calculated transmittances are systematically larger than observed for O_2 lines in agreement with the known 1-4 % underestimation of HITRAN intensity values compared to those of [5,25,27] (see **Fig. 1d** for instance). The largest residuals obtained with "Mendonca2019", "Tran2020" and "Fleurbaey2020" are mainly due to absorption by H_2O (*e.g.* at about 7804.0, 7807.4, 7814.4 and 7830.3 cm^{-1}). This contribution of H_2O absorption will be discussed in the next section. In overall, "Mendonca2019", "Tran2020" and "Fleurbaey2020" lead to relatively close spectral residuals and *rms* values. No particular residuals associated with the differences in the line positions between "Mendonca2019" and the two other datasets (**see Fig. 1a**) can be observed, likely because they are largely compensated by the difference in the pressure-induced line shifts (**Fig. 1b**). In the Q branch region, significant improvements are observed with "Tran2020" and "Fleurbeay2020" with respect to "Mendonca2020". This is likely due to the fact that in these two datasets, line-mixing effects were taken into account for Q-branch lines, while they were neglected in "Mendonca2019". This was confirmed by tests in which the line-mixing coefficients in "Tran2020" were set to zero, all the other parameters remaining the same.

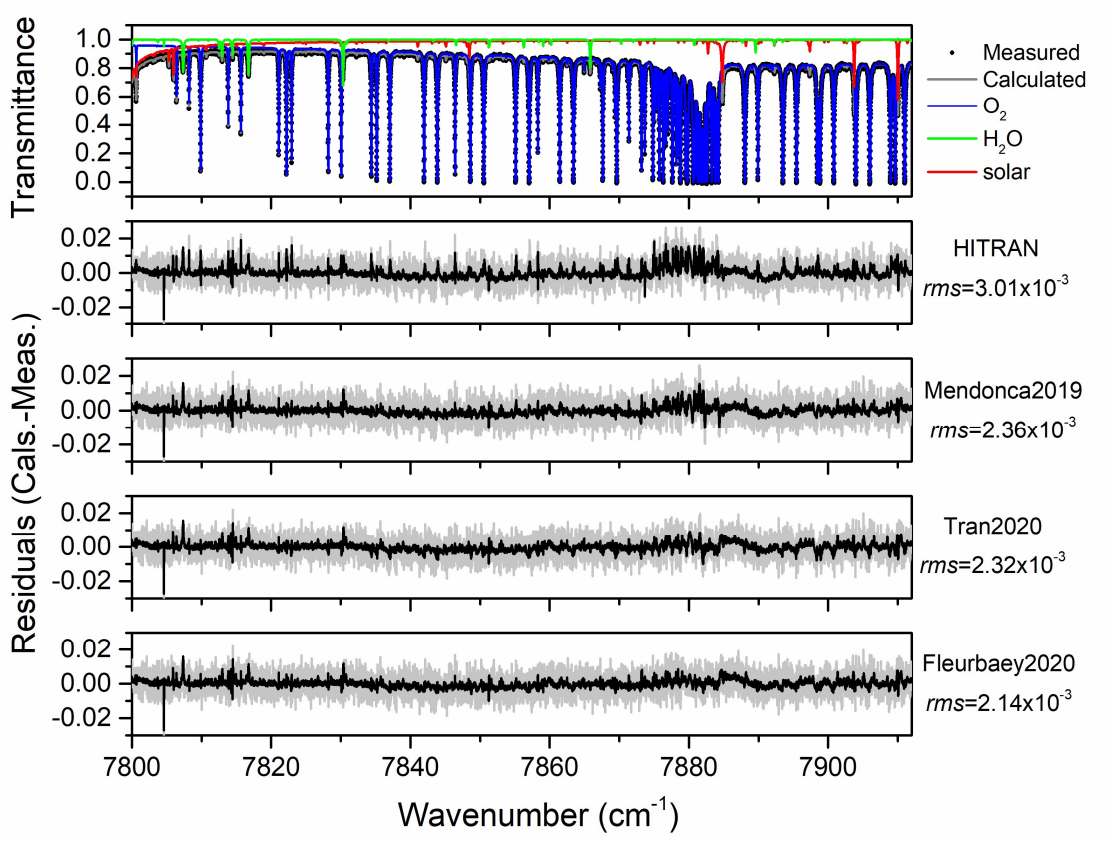

Fig. 3*: The same as for* ***Fig. 2*** *except that in the lower panels, the corresponding "calculated-measured" residuals are plotted in gray, while in black are the "calculated-measured" residuals averaged over 65 situations of close SZA (from 60° to 80°) and humidity (TPW from 0.15 cm to 0.97 cm).*

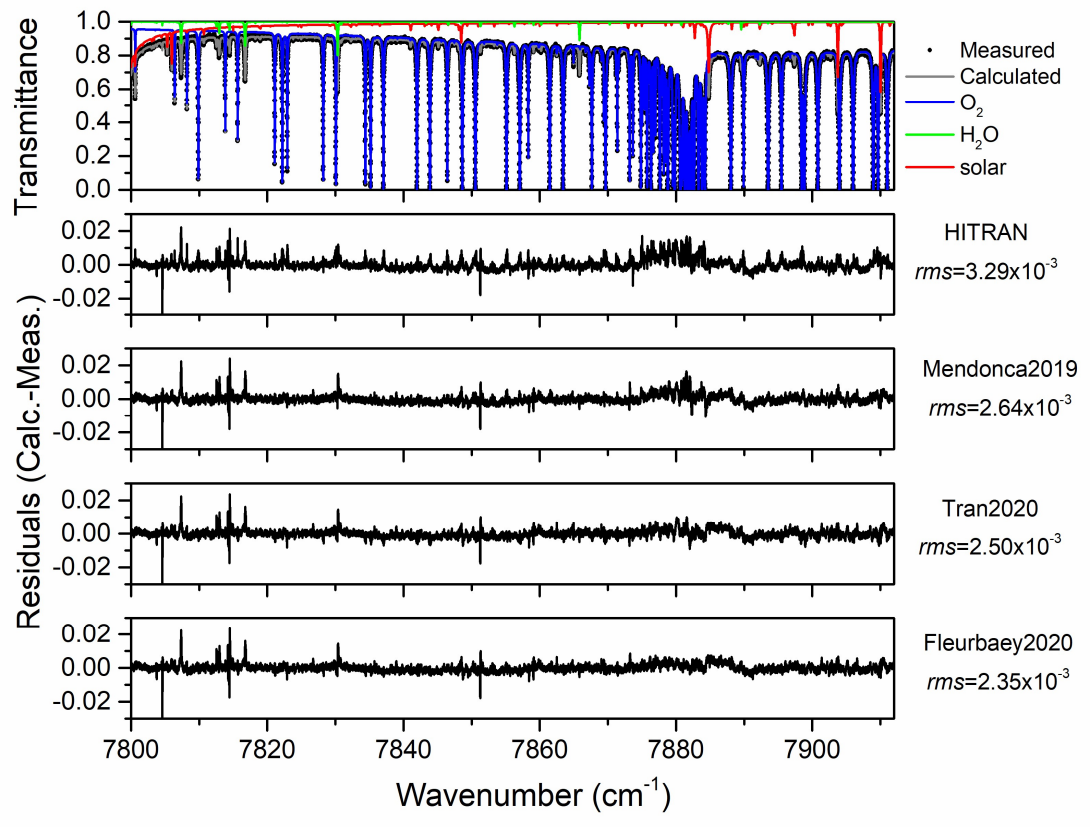

Fig. 4*: Results obtained for the second set involving 40 spectra measured at Caltech. The upper panel shows an example of measured transmission, recorded on 27 January 2017 for a SZA of 69.15° and TPW of 0.73 cm, the corresponding simulated spectrum and the O_2 and H_2O contributions. In the lower panels are plotted the corresponding "calculated-measured" residuals averaged over 40 situations of close SZA (from 60° to 80°) and humidity (TPW from 0.3 cm to 1.19 cm).*

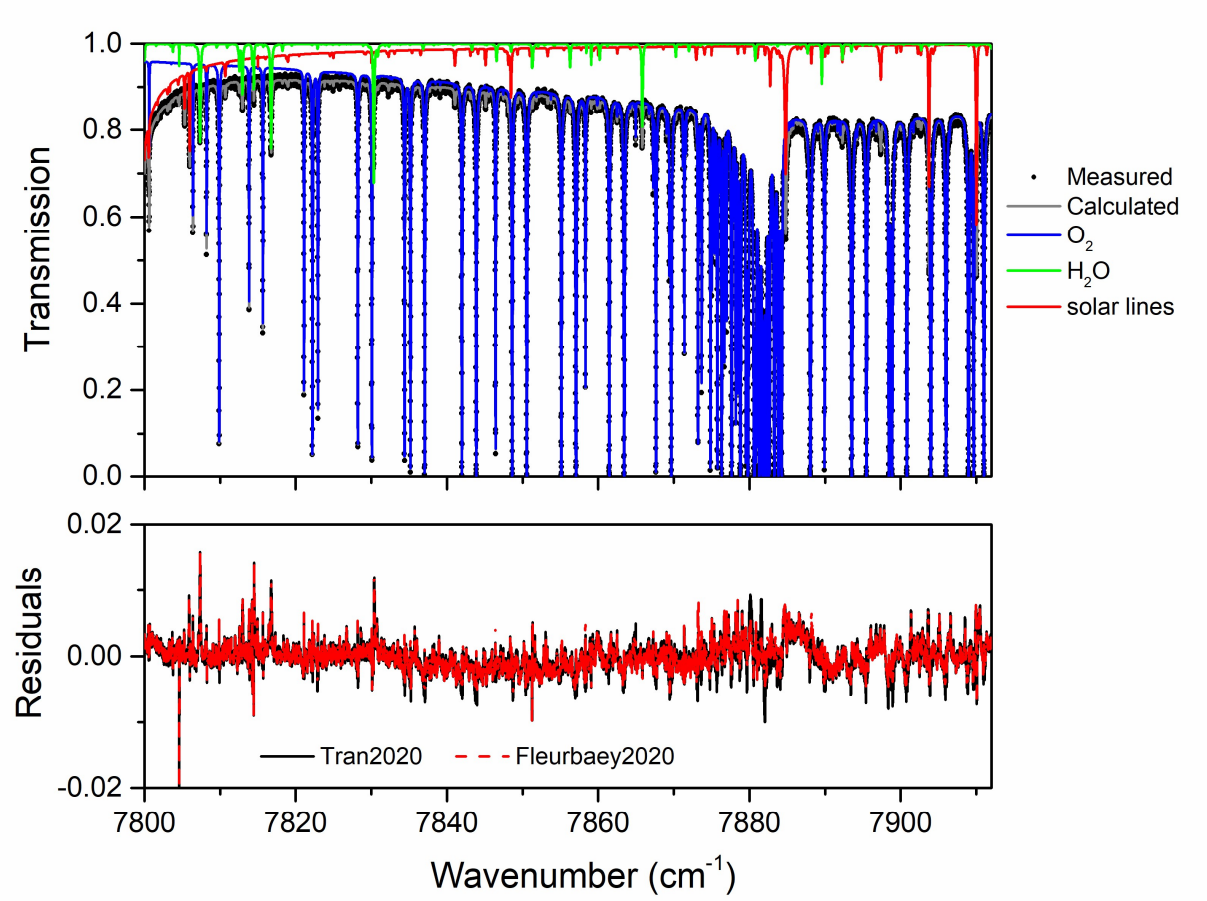

Fig. 5*: Same as* ***Fig. 3*** *except that only residuals corresponding to "Tran2020" and "Fleurbaey2020" are plotted on the lower panel.*

For all the situations that we considered, "Fleurbaey2020" gives the best agreement with measurements. Using the same line-shape model (qsdNG), the spectroscopic parameters of "Fleurbaey2020" and "Tran2020" are quite close, *e.g.* the average ratio between the line intensities of "Tran2020" and "Fleurbaey2020" is 1.0048 (±0.0044) and for the air-broadening coefficient it is 1.0039 (±0.0082). These differences, even though they are very small, lead to differences that can be observed in the spectral residuals plotted in **Figs. 3** and **4** and shown again in **Fig. 5** for better readability. This analysis demonstrates that averaging the "calculated-observed" residuals over a large number of TCCON recordings enables to evidence the impact of small differences in the spectroscopic parameters.

We note that significant (and similar) residuals remain for "Tran2020" and "Fleurbaey2020" simulations (lower panel of **Fig. 5).** They could originate from remaining spectroscopic errors (on the temperature dependences of the line-shape parameters for instance) but they could also be a result of systematic errors in the temperature and pressure profiles as well as on the apparatus functions used in the calculations.

It is worth noting that Mendonca *et al.* used their line list ("Mendonca2019") with the qsdV profile, and data in the TCCON standard analysis software GGG [34] (i.e. data from [2] and [38] with the Voigt profile), to retrieve O_2 atmospheric columns from spectra measured in four TCCON sites [5]. Compared to the GGG data, the "Mendonca2019" dataset was found to only slightly improve the fit residuals but it led to large differences for the retrieved O_2 columns. Therefore, it would be interesting to use the four line lists considered in the present work to study their influence on the retrieved O_2 columns or surface pressures.

3.2 Absorption due to H_2O lines

The third set of spectra which contains 10 spectra measured at Park Falls with solar zenith angles (SZAs) of about 40° but for large humidity conditions (TPW≈2 cm), is used to evaluate the spectroscopy of H_2O absorption lines in the considered spectral region. Notably, large residuals are readily apparent (see **Fig. 6**). Here, simulations were performed using the line set "Tran2020" and the same model for the CIA for O_2 absorption contribution as before. The lower panel of **Fig. 6** shows that the large remaining residuals coincide with water absorption lines. Recall that all previous calculations used the same set of H_2O spectroscopic parameters from GEISA2015 [19]. The shapes of the residuals show that the observed line intensities and/or line shape parameters for several H_2O lines are not accurate. Simulations using HITRAN2016 line parameters for H_2O lead to very similar residuals (lower panel in **Fig. 6**). Tests were also made with the most recent data of H_2O in the 2019 version of the GEISA database [39]. In this spectral region, the GEISA2019 was updated using line intensities and air-broadening and -shifting coefficients provided in the H_2O line list from Mikhailenko *et al.* [40], whereas the line positions were refined using [41]. Note that local discrepancies due to erroneous broadening values of some H_2O lines were identified in [40] and GEISA2015 (for the H_2O line at 7804.6092 cm^{-1} for example), and some air-broadening parameters from GEISA2011 were reintroduced in GEISA2019. A complete description of the changes in GEISA2019 can be found in [39]. For the considered spectral region, GEISA2019 leads to an improvement for the line at 7804.6092 cm^{-1} but most of the other H_2O residuals remain. Tests were made in order to check if these residuals are caused by an erroneous vertical profile of water vapor used as input data for the calculations. To test this hypothesis, the input profile of water vapor concentration was

increased and decreased by 5% and the corresponding calculations were performed. The obtained results show that none of these changes simultaneously reduces the observed residuals for all the H_2O absorption lines. Therefore, these residuals are ascribed to inaccurate spectroscopic data for these H_2O lines. Note that local residuals due to the inaccuracies of spectroscopic parameters of several H_2O lines in this B4 band are expected to have only quite small influence on the surface pressure or air mass retrieved using the whole band. This expectation will be checked in a forthcoming study in which both the B4 and B1 (*i.e.* the O_2 A band region) bands will be used to retrieve the surface pressure or the O_2 columns from ground-based measurements. Nevertheless, if one wants to use the H_2O lines of the region to retrieve the quantity of H_2O, an improvement of H_2O spectroscopic data is required. Note also that no additional residuals from the O_2 absorption lines are observed for these humid spectra when compared with results obtained for dry atmospheres. This can be explained by the fact that, for O_2 lines, H_2O- and air-broadening coefficients have similar values [42,43].

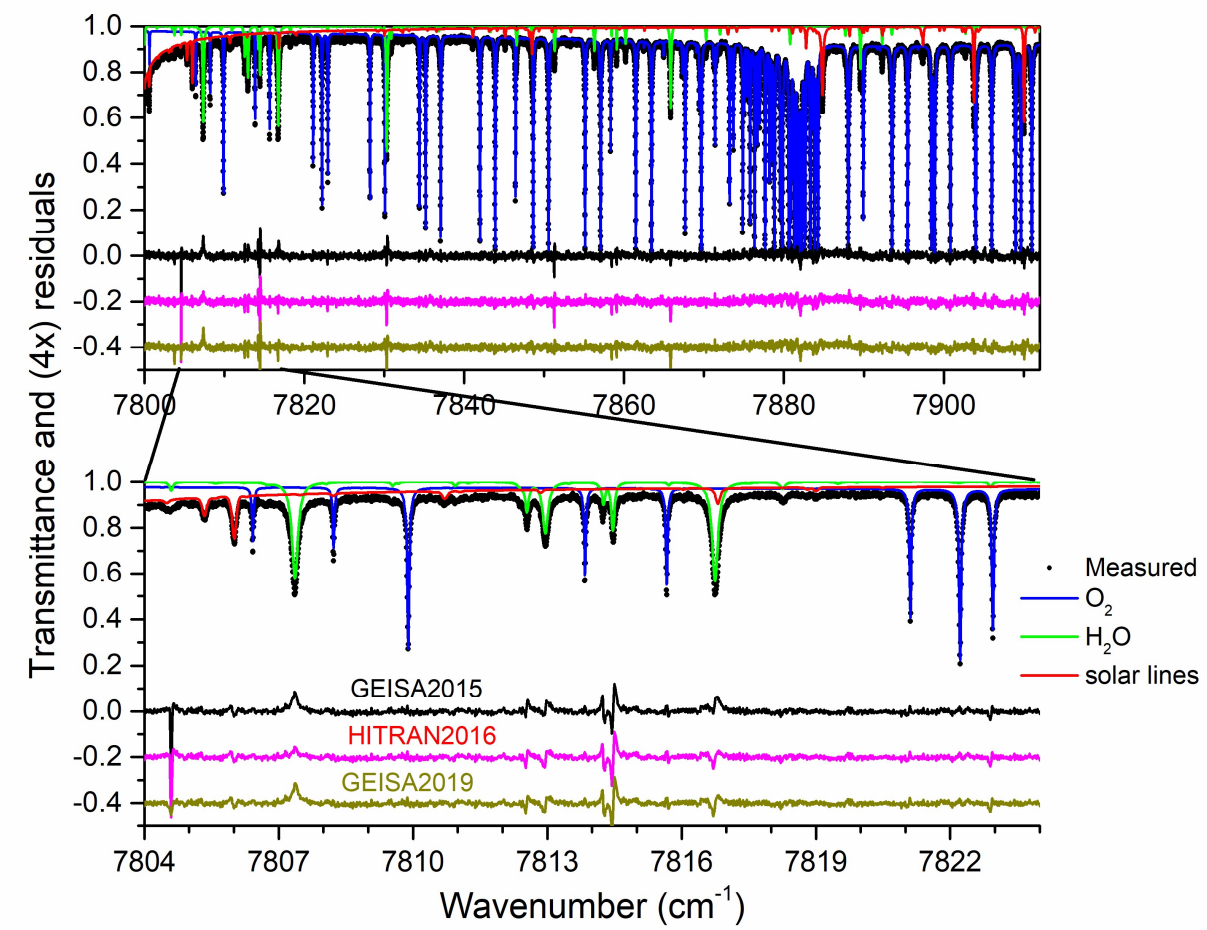

***Fig. 6**: Comparison between an atmospheric spectrum, recorded on September 10, 2007 at Park Falls for a SZA of 41.50° and TPW=2 cm and the corresponding transmission calculated with "Tran2020" dataset [25]. The upper panel shows the comparison for the whole B4 band of MicroCarb while a zoom is presented in the lower panel, H_2O contribution being calculated*

using GEISA2015 [19] line list for this example . The residuals (averaged over 10 spectra of the set and multiplied by 4) in black, red and dark yellow are obtained with data for H_2O absorption lines taken from GEISA2015 [19], HITRAN2016 [11] and GEISA2019 [39], respectively. Residuals obtained with H_2O data from HITRAN2016 and GEISA2019 were shifted along the vertical axis by -0.2 and -0.4.

4. Conclusion

Various sets of absorption line parameters for O_2 in the 1.27 μm spectral region have been evaluated using TCCON atmospheric observations and the SPARTE calculation chain. Averaging the "calculated-observed" residuals over a large number of measurements for similar solar zenith angles and atmospheric humidity conditions enables one to evidence the effect of relatively small spectroscopic data changes, on the spectral residuals. These results show that spectroscopic parameters in the HITRAN2016 and GEISA2015 databases lead to large residuals, while among the most recent studies, the line parameters of [27] and [25] lead to the best agreement with atmospheric measurements. This study also shows that the spectroscopic data available in the HITRAN and GEISA databases for H_2O absorption lines in this spectral region need to be improved. The different datasets tested in the present study will be further evaluated in a forthcoming study in which the surface pressure and/or the total column O_2 amount will be retrieved from atmospheric measurements. It is worth noting that most of the available spectroscopic studies of O_2 in this spectral region were performed at room temperature only. Accurate spectroscopic data for the temperature dependences of both the CIA coefficients and the absorption lines parameters are therefore still needed.

Acknowledgement

Funding from CNES is acknowledged. A large number of TCCON spectra, measured at different sites were made available to us. We would like to thank the PIs of these different TCCON stations. H. Fleurbaey and J. Hodges acknowledge funding from the NIST Greenhouse Gas and Climate Science Program and from the National Aeronautics and Space Administration (NASA) [contract NRA NNH17ZDA001N-OCO2].

References

[1] Long DA, Havey DK, Okumura M, Miller CE, Hodges JT. O_2 A-band line parameters to support atmospheric remote sensing. J Quant Spectrosc Radiat Transf 2010;111:2021-36. doi:10.1016/j.jqsrt.2010.05.011.

[2] Washenfelder RA, Toon GC, Blavier JF, Yang Z, Allen NT, Wennberg PO, Vay SA, Matross DM, Daube BC. Carbon dioxide column abundances at the Wisconsin Tall Tower site. J Geophys Res 2006;111:D22305. doi:10.1029/2006JD007154.

[3] Wunch D, Toon GC, Blavier JF, Washenfelder RA, Notholt J, Connor BJ, et al. The total carbon column observing network. Philos Trans Royal Soc A 2011;369:2087-112. doi:10.1098/rsta.2010.0240.

[4] Sun K, Gordon IE, Sioris CE, Liu X, Chance K, Wofsy SC. Reevaluating the use of O_2 $a^1\Delta_g$ band in spaceborne remote sensing of greenhouse gases. Geophys Res Lett 2018;45:5779-87. doi: 10.1029/2018GL077823.

[5] Mendonca J, Strong K, Wunch D, Toon GC, Long DA, Hodges JT, Sironneau VT, Franklin JE. Using a speed-dependent Voigt line shape to retrieve O_2 from total carbon column observing network solar spectra to improve measurements of x_{CO2}. Atmos Meas Tech 2019;12:35-50. https://doi.org/10.5194/amt-12-35-2019

[6] Bertaux JL, Hauchecorne A, Lefèvre F, Breon FM, Blanot L, Jouglet D, Lafrique P, Akaev P. The use of the O_2 1.27 μm absorption band for greenhouse gas monitoring from space and application to MicroCarb. Atmos Meas Tech 2020;13:3329-74. https://doi.org/10.5194/amt-13-3329-2020

[7] http://www.gosat.nies.go.jp/en/ and references therein

[8] https://oco.jpl.nasa.gov/ and references therein

[9] https://microcarb.cnes.fr/en/MICROCARB/index.htm and references therein

[10] https://amt.copernicus.org/articles/12/1513/2019/

[11] Gordon IE, Rothman LS, Hill C, Kochanov RV, Tan Y, Bernath PF, Birk M, Boudon, Campargue A, Chance KV, Drouin BJ, Flaud JM, Gamache RR, Hodges JT, Jacquemart D, Perevalov VI et al. The HITRAN2016 molecular spectroscopic database. J Quant Spectrosc Radiat Transf 2017;203:3-69. doi: 10.1016/j. jqsrt.2017.06.038.

[12] Maté B, Lugez C, Fraser GT, Lafferty WJ. Absolute intensities for the O_2 1.27 μm continuum absorption. J Geophys Res 1999;104:30,585.

[13] Karman T, van der Avoird A, Groenenboom GC. Line-shape theory of the $X\ ^3\Sigma_g^- \rightarrow a\ ^1\Delta_g, b\ ^1\Sigma_g^+$ transitions in O_2–O_2 collision induced absorption. Journal of Chemical Physics, 2017;147:084307. https://doi.org/10.1063/1.4990662

[14] Karman T, Koenis MAJ, Banerjee A, Parker, DH, Gordon IE, van der Avoird A et al. O_2-O_2 and O_2-N_2 collision-induced absorption mechanisms unraveled. Nature Chemistry, 2018;10, 549–554. https://doi.org/10.1038/s41557-018-0015-x

[15] Mondelain D, Kassi S, Campargue A. Accurate laboratory measurement of the O_2 collision-induced absorption band near 1.27μm. J Geophys Res 2019;124:414-23. doi: 10.1029/2018JD029317.

[16] Yu S, Drouin BJ, Miller CE. High resolution spectral analysis of oxygen. IV. Energy levels, partition sums, band constants, RKR potentials, Franck-Condon factors involving the $X^3\Sigma_g^-$, $a\ ^1\Delta_g$ and $b\ ^1\Sigma_g^+$ states. J Chem Phys 2014;141:174302. https://doi.org/10.1063/1.4900510

[17] Newman SM, Orr-Ewing AJ , Newnham DA , Ballard J . Temperature and pressure dependence of line widths and integrated absorption intensities for the O_2 $a\ ^1\Delta_g - X^3\Sigma_g^-$, (0,0) transition. J Phys Chem 2000;104,42:9467-9480.

[18] Brown LR, Plymate C. Experimental line parameters of the oxygen A band at 760 nm. J Mol Spectrosc 2000;199:166-79.

[19] Jacquinet-Husson N, Armante R, Scott NA, Chédin A, Crépeau L, Boutammine C, Bouhdaoui A, Crevoisier C, Capelle V, Boonne C et at. The 2015 edition of the GEISA spectroscopic database. J Molec Spectrosc 2016;327:31-72.

[20] Hartmann JM, Sironneau V, Boulet C, Svensson T, Hodges JT, Xu CT. Collisional broadening and spectral shapes of absorption lines of free and nanopore-confined O_2 gas. Phys Rev A 2013;87:032510. https://doi.org/10.1103/PhysRevA. 87.032510 2013

[21] Lamouroux J, Sironneau V, Hodges JT, Hartmann JM. Isolated line shapes of molecular oxygen: requantized classical molecular dynamics calculations versus measurements. Phys Rev A 2014;89:042504. https://doi.org/10.1103/PhysRevA.89.042504
[22] Tran DD , Sironneau VT , Hodges JT , Armante R , Cuesta J , Tran H . Prediction of high-order line-shape parameters for air-broadened O_2 lines using requantized classical molecular dynamics simulations and comparison with measurements. J Quant Spectrosc Radiat Transf 2019;222–223:108–14.
[23] Rothman LS, Gordon IE, Babikov Y, Barbe, A, Benner DC, Bernath PF, Birk M, Bizzocchi L, Boudon V, Brown LR, Campargue A, Chance K, Cohen EA, Coudert LH, Devi VM, Drouin BJ et al. The HITRAN2012 molecular spectroscopic database. J Quant Spectrosc Radiat Transf 2013;130:4-50. https://doi.org/10.1016/j.jqsrt.2013.07.002
[24] Konefal M, Kassi S, Mondelain D, Campargue A. High sensitivity spectroscopy of the O_2 band at 1.27 μm: (I) pure O_2 line parameters above 7920 cm^{-1}. J Quant Spectrosc Radiat Transf 2020;241:106653.
[25] Tran DD, Tran H, Vasilchenko S, Kassi S, Campargue A, Mondelain D. High sensitivity spectroscopy of the O_2 band at 1.27 μm: (II) air-broadened line profile parameters. J Quant Spectrosc Radiat Transf 2020;240:106673. https://doi.org/10.1016/j.jqsrt.2019.106673
[26] Rosenkranz PK . Shape of the 5mm oxygen band in the atmosphere. IEEE Trans Antennas Propag 1975;23:498-506.
[27] Fleurbaey H, Hodges JT. Spectroscopic line parameters for air-broadened O_2 lines at 1.27 μm. In preparation.
[28] Armante R, Scott N, Crevoisier C, Capelle V, Crepeau L, Jacquinet N, Chédin A. Evaluation of spectroscopic databases through radiative transfer simulations compared to observations. Application to the validation of GEISA 2015 with IASI and TCCON. J Mol Spectrosc 2016 https://doi.org/10.1016/j.jms.2016.04.004
[29] http://www.noveltis.com/4AOP/
[30] Ngo NH, Lisak D, Tran H, Hartmann JM. An isolated line shape model to go beyond the Voigt profile in spectroscopic databases and radiative transfer codes. J Quant Spectrosc Radiat Transf 2013;129:89-100.
[31] Rohart F, Mader H, Nicolaisen HW. Speed dependence of rotational relaxation induced by foreign gas collisions: studies on CH_3F by millimeter wave coherent transients. J Chem Phys 1994; 101: 6475-86.
[32] Rohart F, Ellendt A, Kaghat F, Mäder H. Self and polar foreign gas line broadening and frequency shifting of CH_3F: effect of the speed dependence observed by millimeter-wave coherent transients. J Mol Spectrosc 1997;185:222-33.
[33] Konefal M, Slowinski M, Zaborowski M, Ciurylo R, Lisak D, Wcislo P. Analytical function correction to the Hartmann-Tran profile for more reliable representation of the Dicke-narrowed molecular spectra. J Quant Spectrosc Radiat Transf 2020;242:106784.
[34] Wunch D, Toon GC, Sherlock V, Deutscher NM, Liu C, Feist DG, Wennberg PO. The Total Carbon Column Observing Network's GGG2014 Data Version. https://doi.org/10.14291/tccon.ggg2014.documentation.R0/1221662, 2015.
[35] CISL RDA: NCEP/NCAR Global Reanalysis Products, 1948-continuing (ucar.edu)
[36] https://www.ecmwf.int/en/forecasts/datasets/reanalysis-datasets/era-interim
[37]Toon GC, "The solar spectrum measured by FTS," in *Imaging and Applied Optics Postdeadline*, OSA Postdeadline Paper Digest (Optical Society of America, 2013), paper FTh1C.3.
[38] Gordon IE, Kassi S, Campargue A, Toon GC. First identification of the electric quadrupole transitions of oxygen in solar and laboratory spectra. J Quant Spectrosc Rad Transf 2010;111:1174-1183. https://doi.org/10.1016/j.jqsrt.2010.01.008.
[39] Armante et al. The GEISA 2019 line spectroscopic parameter database, in preparation.
[40] Mikhailenko SN, Kassi S, Mondelain D, Gamache RR, Campargue A. A spectroscopic database for water vapor between 5850 and 8340 cm^{-1}. J Quant Spectrosc Rad Transf 2016;179:198-216.
[41] Mikhailenko SN, Kassi S, Mondelain D, Campargue A. Water vapor absorption between 5690 and 8340 cm^{-1}: Accurate empirical line centers and validation tests of calculated line intensities. J Quant Spectrosc Rad Transf 2020;245:106840.

[42] Drouin BJ, Payne V, Oyafuso F, Sung K, Mlawer E. Pressure broadening of oxygen by water. J Quant Spectrosc Rat Transf 2014;133:190-198.
[43] Delahaye T, Landsheere X, Pangui E, Huet F, Hartmann JM, Tran H. Measurements of H_2O-broadening coefficients of O_2 A-band lines. J Quant Spectrosc Rat Transf 2014;184:316-321.